Lost, but found with Nile red; a novel method to detect and quantify small microplastics (20 µm–1 mm) in environmental samples

Gabriel Erni-Cassola[1*], Matthew I. Gibson[2,3], Richard C. Thompson[4], Joseph A. Christie-Oleza[1*]

[1] School of Life Sciences, University of Warwick, Coventry CV4 7AL, UK.

[2] Department of Chemistry, University of Warwick, Coventry CV4 7AL, UK.

[3] Warwick Medical School, University of Warwick, Coventry CV4 7AL, UK.

[4] School of Biological and Marine Sciences, Plymouth University, Plymouth PL4 8AA, UK.

*corresponding authors at: School of Life Sciences, University of Warwick, Coventry CV4 7AL, UK.

gabriel.ernicassola@gmail.com / g.ernicassola@warwick.ac.uk and J.Christie-Oleza@warwick.ac.uk

Abstract

Marine plastic debris is a global environmental problem. Surveys have shown that plastic particles <5 mm in size, known as microplastics, are significantly more abundant in surface seawater and on shorelines than larger plastic particles. Nevertheless, quantification of microplastics in the environment is hampered by a lack of adequate high throughput methods to distinguish and quantify smaller size fractions (<1 mm), and this has probably resulted in an underestimation of actual microplastic concentrations. Here we present a protocol that allows high throughput detection and automated quantification of small microplastic particles (20–1000 µm) using the dye Nile red, fluorescence microscopy and image analysis software. This protocol has proven highly effective in the quantification of small polyethylene, polypropylene, polystyrene and nylon 6 particles, which frequently occur in the water column. Our preliminary results from sea surface tows show a power-law increase of small microplastics (*i.e.* <1 mm) with decreasing particle size. Hence, our data helps to resolve speculation on the '*apparent'* loss of this fraction from surface waters. We consider that this method presents a step change in the ability to detect small microplastics by substituting the subjectivity of human visual sorting with a sensitive and semi-automated procedure.

Introduction

It has been estimated that mismanagement of plastic waste resulted in up to 12.7 million tonnes of plastic entering the ocean in 2010 alone.[1] In the environment, plastics accumulate due to their recalcitrant nature, contaminating sediments and surface seawaters on a global scale.[2,3] In aquatic systems, polymer types with lower density than seawater have a higher transportability (*via* rivers[4] into marine coastal areas and oceanic gyres)[5] than higher density polymers, which tend to settle out.[6–8] Lower density plastics, such as polypropylene (PP), polyethylene (PE) and certain forms of polystyrene (PS) are frequently used as packaging materials[9] and hence, have a very short service life prior to disposal. These types of plastic are also more commonly found in environmental surveys.[10,11]

Eriksen *et al.*[12] estimated that about 5.25 trillion plastic fragments are currently floating on the ocean's surface. Extensive sampling of surface seawater and comparison across all size classes (>200 μm) has shown that plastic particles <5 mm are significantly more abundant than larger particles.[5,12,13] These plastic fragments (<5 mm) have been termed microplastics.[14,15] Marine microplastics are composed of two main types: (1) primary microplastics that stem directly from the source, such as microbeads contained in cosmetics, or fibres released during washing of synthetic garments,[16] and (2) secondary microplastics that are generated through macroplastic fragmentation, a break down process influenced by UV-irradiation, high temperatures and mechanical shear forces.[17,18] Morét-Ferguson *et al.*[19], found that the average size of buoyant plastic particles in the Northern Atlantic and Caribbean had halved in size from an average 10 mm in the 1990s to 5 mm in the 2000s. The decrease in average size of plastic marine debris is of concern because the smaller synthetic polymers are ingested by relatively more organisms at the base of the marine food web.[3] Recent studies suggest that ingested particles can be transferred between trophic levels[20,21] and transport persistent organic pollutants.[22] The possible environmental effects of microplastics has led to growing public and media attention as well as policy measures to reduce inputs, such as banning the use of plastic microbeads in personal care products.[23] Besides these concerns and abatement measures, monitoring of marine litter is currently required in the EU under the

Marine Strategy Framework Directive (MSFD)[24] and it is therefore essential to have reliable, reproducible, rapid and inexpensive methods for quantification and monitoring of microplastic contamination in the environment.

Current methodology for quantification of environmental microplastic contamination is hampered by a lack of methods that are both sensitive and allow high throughput quantification. Commonly applied methods separate synthetic microparticles from non-synthetic materials *via* density separation and floatation techniques, before visually sorting the particles and finally confirming their identity with spectroscopy.[25] The data generated can result in an underestimate of small microplastics because of the visual step in the process.[26] Alternative, faster and less expensive protocols are of particular importance for routine monitoring of plastic contamination by regulatory bodies and the need for developing new methods has been clearly identified as a policy priority (MSFD).[24] Here, we adopt the sampling criteria proposed by the EU technical subgroup on marine litter,[24] who recommend two categories: *large* microplastics ranging from 5 mm–1 mm in size (visually recognizable) and *small* microplastics ranging from 1 mm–20 µm for which reliable quantification is still challenging.

In this study, we present the application of a fluorescence-based protocol using Nile red to detect and quantify small microplastics in environmental samples. This method is inexpensive, employs readily available equipment and can be semi-automated for high throughput sample analysis. The method requires a sample purification step, fluorescence microscopy (green fluorescence protein settings) and free image analysis software.

Materials and Methods

Microplastic staining and quantification protocol validation using commercial synthetic polymers

Nile red had been suggested as a tool to fluorescently label microplastics[18,27], and its use was later demonstrated.[28,29] The dye is commonly dissolved in acetone,[30] but here methanol was chosen because common plastics are resistant to it. The fluorescence of Nile red is influenced by its concentration, which lies optimally between 0.1 and 2 µg mL^{-1},[30] and higher concentrations lead to quenching.[30] Accordingly, the working solution for this study was prepared by dissolving Nile red (technical grade, N3013, Sigma-Aldrich) in methanol to a concentration of 1µg mL^{-1}.

Staining efficacy and automated particle detection was tested on nine different polymer types: PE (powder, ~40–48 µm, Sigma-Aldrich), poly(ethylene terephthalate) (PET, powder, ≤300 µm, GoodFellow), PVC (powder, ~80–148 µm, Sigma-Aldrich), nylon 6 (pellets, ~1 mm, Sigma-Aldrich), PP (pellets, ~7 mm, Sigma-Aldrich), PS (pellets, ~5 mm, Sigma-Aldrich), PC (fragment from panel, ~10 mm), polyurethane (PUR, pellets, ~3 mm, Sigma-Aldrich), and black tire rubber (fragment from bicycle tire, 7×4 mm). Nylon 6 microplastics were prepared by heating the pellets and pulling them apart to produce thin fibres, which then were cut to microparticles (~63–91 µm) under a dissection microscope. PP pellets as well as black rubber were ground in liquid nitrogen with mortar and pestle to obtain small microplastic fragments (PP: ~20–130 µm, black rubber: ~57–171 µm). PS and PC microparticles were obtained by sanding the pellets with a metal file and further cutting the obtained particles with a scalpel under a dissection microscope to the final sizes (PS: ~24–196 µm, PC: ~94–169 µm). PUR pellets were directly cut to size under a dissection microscope (~71–154 µm). Sizes of all microparticles produced in the laboratory were calculated from the square root of particle area, which was measured in ImageJ using brightfield microscope images. Ten particles of each polymer type were placed on separate clean PC track-etched

filter membranes (PCTE, 25 mm diameter, 10 µm pore size, Whatman) to evaluate the efficiency of detection of our protocol. PCTE filters are optimal for two reasons: (1) their hydrophilic surface avoids Nile red background fluorescence and (2) translucent properties when exposed to methanol allow brightfield microscopy in addition to fluorescence microscopy. About 2–3 drops of Nile red solution were carefully added to cover each filter. Filters were placed on standard microscope slides, covered with cover slips and fixed with tape to avoid movement of the sample. The samples were then maintained for 10 minutes at 60 °C in the dark.

Microscopic imaging was performed using a light microscope (Nikon Eclipse Ti) equipped with a widefield camera (Andor Zyla sCMOS) and a LED for fluorescence. We tested the fluorescence of the nine different polymers stained with Nile red on PCTE filters in green (excitation/emission 460/525 nm) and red (565/630 nm). Green fluorescence was chosen over red fluorescence because (1) synthetic polymers either fluoresced better in green (fig. S1 a-d) or fluorescence did not differ significantly (fig. S1 e), (2) natural contaminants fluoresced in red but not in green after hydrogen peroxide (H_2O_2) digestion (fig. S2, discussed below) and (3) background signal from the filter membrane was lower. Three types of whole filter images were obtained for each polymer type: red and green fluorescence, as well as brightfield, all at a magnification of 10×. Exposure time for fluorescence was 30 ms at 30% LED strength.

Automated particle recognition and quantification based on the fluorescent images was performed in ImageJ (v1.50i). A macro was written to perform the following tasks: (1) set the scale, (2) substract the background using a rolling ball radius of 1500 pixels, (3) convert images to 8bit, (4) adjust black and white thresholds using 29 and 175 as the lower and higher values of pixel brightness, and finally (5) quantify particles based on area (400 – ∞ µm^2). The size detection limit was set to 400 µm^2 to ensure that pores from the filter membrane (diameter = 10 µm) did not interfere in particle measurements.

Validation of the pre-staining digestion protocol

To prevent overestimation of synthetic particles in environmental samples, it is of critical importance that biogenic materials, such as lipids, chitin or wood lignin, which fluoresce when stained with Nile red (fig. S2 a, c), are eliminated or cease to fluoresce when stained. While digestion with nitric acid proved highly efficient at removing biogenic matter, its application is limited due to pH-sensitive polymers, such as PS particles, which melt together, or Nylon fibres, which are lost during the process.[31] A chemical alternative is given with H_2O_2 treatments, against which common synthetic polymers are resistant.[31,32] Hence, digestion of biogenic material was performed as previously described by Claessens *et al.* with slight modifications.[31] Briefly, 20 ml of 30% H_2O_2 was added to 250 mL Erlenmeyer flasks containing the filtered samples on PCTE filters, which were then kept at 60 °C for 1 h followed by a prolonged 7 h step at 100 °C. Following the digestion, PCTE filters were thoroughly rinsed with Milli-Q water and then removed. The remaining solution was filtered through a new PCTE filter rinsing all particles from the flask and filtering device with Milli-Q water. The new PCTE filter containing all collected material was stored in Petri dishes until Nile red analysis.

The effect of the H_2O_2 digestion protocol on natural polymers was tested with the two most commonly occurring natural polymers: chitin (powder, Sigma-Aldrich) and wood lignin (below 1 mm in size; kindly provided by Prof. Tim Bugg and prepared according to literature).[33]

Validation of the fluorescent-staining protocol with environmental samples

Net tow and beach sand samples were obtained in June 2016 to test our fluorescent-labelling method with environmental samples. Tow samples were collected from within Plymouth Sound, UK. Five consecutive trawls of 15 min were undertaken with a manta net (0.50 m by 0.15 m mouth, 300 µm mesh) at a ship speed of 4 knots. After each tow, the collected material was transferred into a container by rinsing the net and cod end with seawater. In the

laboratory, all material was pre-filtered through a 1 mm metallic mesh to eliminate large debris. Retained debris was thoroughly washed with Milli-Q water to extract all small microplastics. Retained debris was visually examined for plastic debris (fig. S3). The flow through containing plastic particles <1 mm was vacuum filtered through PCTE filters (47 mm diameter, 10 µm pore size, Whatman). All filters were placed into a 250 mL flask.

Sediment samples were collected from a beach at Bigbury (UK, 50°16´53N, 3°53´42W) by transferring the top 1 cm layer of five 30 x 30 cm^2 plots with a metallic spoon into 500 mL glass bottles. Microplastics were extracted from sand samples according to the density-separation/floatation protocol described in Nuelle *et al.*[34] using NaCl (26% w/v) instead of NaI. The collected supernatant was vacuum filtered through PCTE filters, which were placed in a 250 mL flask. Flasks containing the PCTE filters from net tows and beach sand samples were stored at 60 °C during 24 h for desiccation. The H_2O_2 digestion, staining and imaging was performed as described above.

Micro-Raman spectroscopy was used to verify the identity of the fluorescing and non-fluorescing particles found on the filters in order to ascertain the specificity of Nile red to only stain particles of synthetic origin. In total, 23 fields (23 × 1.8 mm^2) from 6 different filter sections (4 sediment samples, 2 water samples) were imaged as described above. Raman spectra were acquired using an inVia Raman microscope (Renishaw). Raman shifted spectra were recorded using a 442 nm excitation laser in a range of 100 to 3500 waves cm^{-1} and 10 s exposure time accumulating 20 scans. Particles were bleached during 5 min prior to spectrum acquisition as Nile red fluorescence interfered with the Raman signal. The baselines of Raman spectra were corrected in R (v3.2.3)[35] using the peak detection method from the baseline package[36] and then normalized.

To control for procedural contamination, Milli-Q water was processed in equal conditions as described above for environmental samples. To avoid lab contamination, lab coats were worn during all procedures, slides were washed with acetone, other glassware and filtering devices were thoroughly rinsed with Milli-Q water, pristine plasticware was used (see supplied protocol regarding required precautions during sample handling, such as

avoiding low quality pipette tips; fig S4), and Nile red staining solution was freshly filtered through 0.2 µm filters.

Data analysis

Automated quantification of fluorescing particles from tow and blank samples was performed in ImageJ using the macro described above. For each sample type, green fluorescence images (109 total) were randomly taken from 5 different filters. Two power-law models were fitted to the particle size distribution with poweRlaw[37] in R. Different x_{min} values were used to estimate the scaling factor: either (1) the smallest particle present in the dataset or (2) an estimate at which the probability distributions of the particle size distribution and the best-fit power-law were most similar above x_{min}.[38] The latter discards particles below the estimated x_{min} for which the power-law model is not valid. Testing for other distributions capable of explaining our data was done in accordance with Clauset *et al.*[38] Plotting was performed in R using the package ggplot2.[39]

A detailed protocol and the code for the macro to semi-automatically quantify fluorescent microplastics in ImageJ are available as supplementary materials.

Results

Validation of the automated Nile red protocol using commercially available plastics

Fluorescence assisted counting. Polymers PE, PP, PS, nylon 6, PC, PET, PVC and PUR fluoresced in green after staining with Nile red (fig. 1) demonstrating the utility of Nile red to detect and quantify small microplastics. Tire rubber did not fluoresce (fig. S1 f). Visual quantification can be performed directly under a microscope, but the implementation of a macro to automate counts allows high throughput counting as well as rapid measurement of the plastic particles. Here, fluorescence based automated detection of microplastics on PCTE membranes was 100 % for 4 polymer types (*i.e.* PE, PP, PS and nylon 6) as all 10 particles of each respective polymer were detected with ImageJ using 29 as the lower threshold for pixel brightness (fig. 1). The other 4 polymers (PUR, PC, PVC and PET) fluoresced weaker and a lower threshold value for pixel brightness (*i.e.* 9) was required to automatically detect all 10 particles (fig. 1).

As fluorescence intensity varied with polymer type and thickness, the original setting for the pixel brightness threshold (*i.e.* 29) in our macro for ImageJ was optimized to capture all particles with strong fluorescence (*i.e.* PE, PP, PS and nylon 6), and to represent particle size accurately, using brightfield images as size references (figs. 1 & 2). As stated above, 100% detection of PUR, PC, PET, and PVC was achieved by lowering the threshold value for pixel brightness. However, the adoption of the lower threshold (1) overestimated the size of more strongly fluorescing particles (*i.e.* PE, PP, PS and nylon 6 in fig. 2), (2) counted strongly fluorescent particles in very close proximity as one unique particle, and (3) so increased the risk of false positives (*i.e.* chitin in fig. 1; discussed below).

Implementation of the fluorescent-staining protocol to environmental samples

Digestion of biogenic material. Wood lignin fluoresces green and red when stained with Nile red (fig. S2 a). However, particles of this natural polymer, which are below 1 mm in size,

were completely eliminated after applying a 7-hour H_2O_2 digestion protocol (fig. S2 b). As with wood lignin, chitin also fluoresces in green and red when stained with Nile red (fig S2 c), but was not completely removed during the 7 hour H_2O_2 treatment. Interestingly, after digestion, chitin showed a strong decrease in green fluorescence intensity (but not red fluorescence; fig. S2 d), possibly due to reduced hydrophobicity in response to oxidation. To test whether chitin would interfere with the detection and quantification of synthetic polymers in the green spectrum, we performed our protocol on a mix of chitin and PE. A stark distinction between PE particles and chitin was observed (fig S2 e–g) as the weak fluorescence given by chitin did not interfere when using our highly stringent macro settings (pixel brightness of 29), but chitin is detected to some extent when the settings are brought down (pixel brightness 9). This result highlights two issues that need to be considered when using this protocol: (1) Nile red strongly fluoresces under the GFP settings when staining highly hydrophobic plastics (such as PE, PP, PS) and, hence, green fluorescence should be used to eliminate background and inclusion of natural contaminants; and (2) reducing the sensitivity for the detection of less hydrophobic plastics (e.g. PC, PVC, PUR and PET) can come with a risk of including the detection of particles of natural origin.

Detection and quantification of microplastics in environmental samples. Here we isolated microplastics from environmental samples (*i.e.* beach sediment and sea surface) with saturated NaCl solutions and, hence, expected to extract plastics with densities ≤1.2 g/cm^3 (*e.g.* PE, PP, PS and nylon 6). We applied our Nile red staining protocol to discriminate small microplastic particles from other materials based on fluorescence (fig. 3) as well as to quantify and measure them. The automated ImageJ quantification of microplastics from the sea surface samples using stringent settings resulted in a total of 199 fluorescent particles, ranging between 20 – 338 µm in size (*i.e.* particle size was obtained from the square root of the area measured for each individual particle; fig. 4). Neither of the power-law models describing the data could be dismissed ($p_{x.min = 20.02} = 0.72$ and $p_{x.min = 101.76} = 0.85$). The particle size distribution followed a power-law more closely for particles >101 µm, than if all data

were used, *i.e.* the smallest particle size = 20 µm (see table S1 for statistical details). The calculated scaling factors were 2.13 for x_{min} = 20.02 and 4.42 for x_{min} = 101.76.

Only one fluorescent particle was detected in our negative controls (*i.e.* processed Milli-Q water) demonstrating that laboratory contamination was minimal. It is of uttermost importance to include controls in order to assess the contamination acquired during the processing of samples.

For this protocol to be effectively applied to environmental samples we realise it is critical that *only* plastic particles should fluoresce and, hence, be quantified with the semi-automated process. Consequently, we scanned *via* Raman spectroscopy a total of 60 fluorescing and non-fluorescing particles and found that all of the fluorescing particles (n = 37) were of synthetic origin, while all non-fluorescing particles (n = 23) gave *non-plastic* Raman signatures (*e.g.* fig. 3). The environmental samples predominantly contained PP-type polymers (83.8%), although PE was also found (16.2%). The Raman spectra of the PP and PE particles contained slight variations in peak structure (fig. S5), which can occur in commercial polymer materials due to the inclusion of additional compounds and pigments or as a consequence of environmental weathering.[40]

Discussion

We present a fast, reliable and cost-effective method for detecting, quantifying and determining the size of small PE-, PP-, PS- and nylon 6 type microplastics (20 µm – 1 mm) commonly present in sea surface samples.[10,11,41] This method uses the lipophilic dye Nile red to fluorescently label plastics and requires fluorescence microscopy to capture images at magnification 10× prior to automated, image-based quantification in ImageJ using a macro (both protocol and macro are provided as supplementary information) enabling high throughput image analysis. Specific protocols for collecting and extracting microplastics from the environment were not in the scope of this work.

During the preparation of this manuscript, two studies were published[28,42] that reasserted our findings, demonstrating the effectiveness of Nile red to fluorescently label different types of commercially available synthetic polymers, such as the ones employed here, all of which fluoresce in the green spectrum (black rubber was not used in these previous studies and we show here that it does not fluoresce). Indeed, similarly to us, Shim *et al.*[28] concluded that green-yellow fluorescence (excitation/emission 450–490/515–565 nm) provided better particle recognition than red or blue fluorescence. Using a different light and filter set-up, Maes et al.[42] reported good fluorescence at longer wavelengths ranging from yellow to orange, depending on the polymer type. Such findings agree with previous reports about the behaviour of Nile red, which favours detection of strongly hydrophobic samples at short excitation/emission wavelengths (450–500/≤580 nm) compared to more neutral lipids, which should ideally be visualised at longer excitation wavelengths (*i.e.* red, 515–560/≥590 nm).[30] For example, given that PE and PP are more hydrophobic than PET,[43] it is expected that the former will fluoresce more intensely at shorter wavelengths (*i.e.* green), while their fluorescence at longer wavelengths remains weak or even absent as we show in figure S1. We are therefore confident that the Nile red protocol we propose here is effective in detecting strongly hydrophobic plastics such as PE, PP, PS and nylon 6 through the use of GFP settings (green fluorescence), while preventing detection of contaminants, that would fluoresce at

longer wavelengths. We acknowledge the protocol's limitations for the less hydrophobic polymers PC, PUR, PET and PVC, which constituted about 25% of the European plastic demand in 2015.[9] These limitations can to some extent be overcome as suggested in the results section by increasing the sensitivity of the method (fig. 1), but this comes at a risk of overestimating the size of strongly fluorescent polymers (fig. 2) as well as incurring the possibility of false positives, such as chitin. It is also worth highlighting that all polymer types that fluoresced weakly in our study when stained with Nile red (PC, PUR, PET, PVC) are denser (≥1.2 g/cm^3) than the polymers that fluoresced more strongly (PE, PP, PS, nylon 6, <1.08 g/cm^3). Hence, the latter can be extracted using a saturated NaCl solution as done in this study, while denser polymers would require a higher density salt solution (*e.g.* NaI).

The successful application of a Nile red protocol to environmental samples relies on the efficient removal of biogenic particles that could be detected as false positives. As we show here, abundant natural polymers such as chitin and wood lignin fluoresced when stained with Nile red (fig. S2 a, c). Shim *et al.*[28] remained cautious on applying Nile red to quantify microplastics in environmental samples due to the risk of co-staining undigested biogenic material. We speculate that the problem they encountered resided in the weak digestion treatment they applied on their beach samples (*i.e. soaking* the filters with 35% H_2O_2), which resulted in biogenic debris such as an amphipod carapace and plant parts still being present. In turn, Shim *et al.*[28] reported less such contamination for the neuston net samples, which were digested with the more aggressive Fenton reagent (including heating to 75°C). Hence, a harsh digestion protocol such as the one we used here and which was previously suggested by Claessens *et al.*[31], is required to prevent co-staining of natural organic polymers and confidently quantify Nile red-stained microplastics in environmental samples. Common plastics such as PE, PP, PS, PET and nylon 6 are resistant to H_2O_2, as demonstrated by Tagg *et al.*[32] during a 7-day exposure experiment, where no significant chemical changes were detected *via* FTIR, as opposed to alterations observed elsewhere that were induced by solvents such as acids and bases (e.g. HCl or NaOH).[34,44] In addition to the H_2O_2 digestion, we propose to include a 1 mm mesh-size sieving step prior to the digestion to prevent the

346 inclusion of larger, hard-to-digest natural contaminants, such as amphipods or pieces of
347 wood. If required, enzymatic digestion protocols could be implemented to digest biota-rich
348 environmental samples.[4,44] Indeed, sample purification may further be optimized by
349 combining digestion procedures with a density separation protocol, such as presented by
350 Maes et al.[42] Nevertheless, our results show how the 30% H_2O_2 digestion step used here was
351 effective at preventing detection of small natural polymers (below 1 mm in size); wood lignin
352 was completely degraded and chitin was no longer was detectable in ImageJ using green
353 fluorescence images (fig S2). Furthermore, we successfully proved that all of the fluorescing
354 particles from environmental samples assessed with micro-Raman spectroscopy (n = 37) were
355 identified as synthetic plastic materials, whereas no non-fluorescing particles scanned (n =
356 23) showed a synthetic polymer signature.

357 Other semi-automatable methods to detect and quantify small microplastics in
358 environmental samples were recently developed:[32,45,46]

359 Chemical mapping *via* micro-FTIR was shown useful to detect and identify small
360 microplastics directly on filters when combined with FPA detectors;[32,45] FPA detectors can
361 record several thousand spectra simultaneously and plastics are then identified based on
362 characteristic bands that are shared by synthetic polymers. However, access to such
363 specialised pieces of equipment is not always possible, and the time required to image a
364 whole filter membrane (10.75 h for a 25 mm diameter filter)[45] is significantly higher than
365 when using the method in the present study *i.e.* 20 min.

366 A second semi-automatable approach used to detect small microplastics from
367 environmental samples combined Micro-Raman spectroscopy with particle finding
368 software.[46] The software provides geographical positions of the particles on a slide, and the
369 particles are then scanned individually *via* a motorised stage. However, Frère *et al.*[46] did not
370 apply this technique directly to the sample filter (such as in this study and others[32,45]). Instead,
371 particles were visually pre-selected under a dissection microscope and then transferred onto a
372 gold-coated microscope slide. It is therefore not yet clear whether this technique is also
373 applicable to quantify small microplastics without potentially introducing visual bias.

While our Nile red staining method does not provide the chemical identity of the detected plastic particles (as achieved *via* FTIR and Raman), we present it as a sensitive, cost-effective and unbiased way of quantifying and measuring small PE, PP, PS and Nylon 6 particles in environmental sample preparations to acquire large datasets with high statistical value. Ultimately, a fraction of pinpointed plastic particles should be identified *via* micro-Raman spectroscopy to obtain information on the diversity of polymer types within a sample. Moreover, despite having tested the most common potential natural contaminants, we advocate the use of micro-Raman spectroscopy on subsamples until full reliability of the method presented here has been evaluated.

Micro-Raman spectroscopy of plastic particles detected with Nile red showed that PP microparticles were more prevalent (83.8%) in our environmental samples than PE (16.2%). This is notable as PE is the most commonly produced polymer type[47] and literature highlights PE as the most abundant polymer on sea surfaces.[48] A recent study, however, found that this is only the case for large microplastics (>1 mm), as the smaller analysed size fraction (0.335 – 1 mm) was dominated by PP (42%) rather than PE (26%).[46] Furthermore, the authors reported a lack of PS in size classes below <2 mm,[46] which resembles our findings. Curiously, PS was present in the fraction retained by the 1 mm sieve (fig. S3) but not found among particles assessed with Raman. Several non-exclusive hypotheses may explain these findings. For instance, fragmentation behaviours may differ with polymer type and shape. Particles have also been observed to adhere to organic matter, such as marine snow, and sink.[49,50] It is unclear, however, why small PE particles would more likely be incorporated into marine snow than PP particles, and further research is required to shed light on this interesting phenomenon.

Plastics in the environment are known to progressively fragment into smaller particles.[2] Based on the fragmentation pattern of three dimensional objects, it could be expected that the abundance of microplastic particles increases following a power-law with a factor of 3 as size decreases.[5] Contrary to this assumption, Cózar *et al.*[5] reported an intriguing loss in abundance of small microplastics after carrying out a global survey of sea surface

marine plastic debris. The expected correlation between size and fragment abundance was observed down to a particle size of 2 mm but, surprisingly, the abundance of microplastics sharply decreased for particles below 1 mm in size. This supported speculation regarding the substantial 'missing' fraction of marine plastic debris initiated in 2004,[14] and recently reviewed by Eriksen *et al.*[51] We believe that the extremely low incidence of small microplastics reported by Cózar *et al.*[5] may partly be ascribed to the methods employed in identifying and selecting particles, which were based on visual sorting under a dissecting microscope. In fact, in a study whose findings mirrored our own, Enders *et al.*[52] showed that small microplastics were indeed present in surface waters with increasing abundance as size decreased, and obtained a scaling factor of 1.96 for the size range of 10 – 110 µm, close to one obtained in this study (*i.e.* scaling factor of 2.13). Further research is nevertheless required, as very little is known about the fragmentation pattern and particle behaviour of different polymer types in the marine environment.[53]

Here we suggest the use of a highly sensitive Nile red fluorescent staining method for identifying the smaller size range of lower density microplastics (<1 mm) commonly present in sea surface samples (*i.e.* PE, PP, PS and nylon 6). We acknowledge its limitations, but do not exclude its application, for less hydrophobic polymer types, a separation that coincides with higher polymer densities (>1.2 g/cm^3; fig. 1). Using this time- and cost-effective protocol to quantify and measure small microplastics allowed us to confirm that small microplastics are increasingly abundant with decreasing particle size in sea surface samples (fig. 4). This method therefore addresses the quantification uncertainties and provides an effective tool for rapid quantification of small microplastics by substituting the visual selection and quantification process with an automated process.

Supporting Information

Five figures (green and red fluorescence, Nile red stained natural polymers, microplastics >1 mm, contamination control, example Raman spectra of microplastics from environmental

429 samples), one table with statistical details, a sample preparation protocol and the code for the

430 ImageJ script used to quantify fluorescent microplastic particles; all as noted in the text

431
432

Acknowledgements

This work was supported by the NERC Independent Research Fellowship NE/K009044/1. The microscope facility was provided by WISB, which is a BBSRC/EPSRC Synthetic Biology Research Centre (grant ref.: BB/M017982/1) funded under the UK Research Councils' Synthetic Biology for Growth programme. Gabriel Erni Cassola was supported by a NERC CENTA PhD studentship. We thank skipper Richard Ticehurst (Plymouth University) for his help and expertise during field work. Special thanks go to Vinko Zadjelovic and Robyn Wright for providing input throughout the study. The authors declare no conflict of interest.

Author contributions

G.E.C., J.C.-O. and M.I.G. conceived the study. G.E.C. designed and conducted the experimental work. R.C.T. provided expertise and advice on fieldwork, microplastic identification and gave access to the facilities. G.E.C. and J.C.-O. analysed the data and wrote the paper. M.I.G. and R.C.T. provided their expertise and reviewed the manuscript.

References

(1) Jambeck, J. R.; Geyer, R.; Wilcox, C.; Siegler, T. R.; Perryman, M.; Andrady, A.; Narayan, R.; Law, K. L. Plastic waste inputs from land into ocean. *Science (80-.).* **2015**, *347* (6223), 768–771.

(2) Barnes, D. K. A.; Galgani, F.; Thompson, R. C.; Barlaz, M. Accumulation and fragmentation of plastic debris in global environments. *Phil. Trans. R. Soc. B* **2009**, *364*, 1985–1998.

(3) Wright, S. L.; Thompson, R. C.; Galloway, T. S. The physical impacts of microplastics on marine organisms: A review. *Environ. Pollut.* **2013**, *178*, 483–492.

(4) Mani, T.; Hauk, A.; Walter, U.; Burkhardt-Holm, P. Microplastics profile along the Rhine River. *Sci. Rep.* **2015**, *5*, 17988.

(5) Cózar, A.; Echevarría, F.; González-Gordillo, J. I.; Irigoien, X.; Ubeda, B.; Hernández-León, S.; Palma, A. T.; Navarro, S.; García-de-Lomas, J.; Ruiz, A.; et al. Plastic debris in the open ocean. *PNAS* **2014**, *111*, 10239–10244.

(6) Woodall, L. C.; Sanchez-Vidal, A.; Canals, M.; Paterson, G. L. J.; Coppock, R.; Sleight, V.; Calafat, A.; Rogers, A. D.; Narayanaswamy, B. E.; Thompson, R. C. The deep sea is a major sink for microplastic debris. *R. Soc. Open Sci.* **2014**, *1* (4), 140317.

(7) Claessens, M.; Meester, S. De; Landuyt, L. Van; Clerck, K. De; Janssen, C. R. Occurrence and distribution of microplastics in marine sediments along the Belgian coast. *Mar. Pollut. Bull.* **2011**, *62* (10), 2199–2204.

(8) Pedrotti, M. L.; Petit, S.; Elineau, A.; Bruzaud, S.; Crebassa, J.-C.; Dumontet, B.; Martí, E.; Gorsky, G.; Cózar, A. Changes in the Floating Plastic Pollution of the Mediterranean Sea in Relation to the Distance to Land. *PLoS One* **2016**, *11* (8), e0161581.

(9) PlasticsEurope. Plastic - the facts 2016. *Brussels* **2016**.

(10) Suaria, G.; Avio, C. G.; Mineo, A.; Lattin, G. L.; Magaldi, M. G.; Belmonte, G.; Moore, C. J.; Regoli, F.; Aliani, S. The Mediterranean Plastic Soup: synthetic polymers in Mediterranean surface waters. *Sci. Rep.* **2016**, *6*, 37551.

(11) Gajšt, T.; Bizjak, T.; Palatinus, A.; Liubartseva, S.; Kržan, A. Sea surface microplastics in Slovenian part of the Northern Adriatic. *Mar. Pollut. Bull.* **2016**, *113*, 392–399.

(12) Eriksen, M.; Lebreton, L. C. M.; Carson, H. S.; Thiel, M.; Moore, C. J.; Borerro, J. C.; Galgani, F.; Ryan, P. G.; Reisser, J. Plastic Pollution in the World's Oceans: More than 5 Trillion Plastic Pieces Weighing over 250,000 Tons Afloat at Sea. *PLoS One* **2014**, *9* (12), e111913.

(13) Cózar, A.; Sanz-Martín, M.; Martí, E.; González-Gordillo, J. I.; Ubeda, B.; Gálvez, J. Á.; Irigoien, X.; Duarte, C. M. Plastic Accumulation in the Mediterranean Sea. *PLoS One* **2015**, *10* (4), e0121762.

(14) Thompson, R. C.; Olsen, Y.; Mitchell, R. P.; Davis, A.; Rowland, S. J.; John, A. W. G.; McGonigle, D.; Russell, A. E. Lost at sea: where is all the plastic? *Science (80-.).* **2004**, *304* (5672), 838.

(15) Moore, C. J. Synthetic polymers in the marine environment: A rapidly increasing, long-term threat. *Environ. Res.* **2008**, *108*, 131–139.

(16) Browne, M. A.; Crump, P.; Niven, S. J.; Teuten, E.; Tonkin, A.; Galloway, T.; Thompson, R. Accumulation of microplastic on shorelines woldwide: Sources and sinks. *Environ. Sci. Technol.* **2011**, *45* (21), 9175–9179.

(17) Corcoran, P. L.; Biesinger, M. C.; Grifi, M. Plastics and beaches: A degrading relationship. *Mar. Pollut. Bull.* **2009**, *58* (1), 80–84.

(18) Andrady, A. L. Microplastics in the marine environment. *Mar. Pollut. Bull.* **2011**, *62* (8), 1596–1605.

(19) Morét-Ferguson, S.; Lavender, K.; Proskurowski, G.; Murphy, E. K.; Peacock, E. E.; Reddy, C. M. The size, mass, and composition of plastic debris in the western North Atlantic Ocean. *Mar. Pollut. Bull.* **2010**, *60*, 1873–1878.

(20) Setälä, O.; Fleming-Lehtinen, V.; Lehtiniemi, M. Ingestion and transfer of microplastics in the planktonic food web. *Environ. Pollut.* **2014**, *185*, 77–83.

(21) Watts, A. J. R.; Lewis, C.; Goodhead, R. M.; Beckett, S. J.; Moger, J.; Tyler, C. R.; Galloway, T. S. Uptake and Retention of Microplastics by the Shore Crab Carcinus maenas. *Environ. Sci. Technol.* **2014**, *48* (15), 8823–8830.
(22) Teuten, E. L.; Saquing, J. M.; Knappe, D. R. U.; Barlaz, M. A.; Jonsson, S.; Björn, A.; Rowland, S. J.; Thompson, R. C.; Galloway, T. S.; Yamashita, R.; et al. Transport and release of chemicals from plastics to the environment and to wildlife. *Philos. Trans. R. Soc. B* **2009**, *364*, 2027–2045.
(23) Rochman, C. M.; Kross, S. M.; Armstrong, J. B.; Bogan, M. T.; Darling, E. S.; Green, S. J.; Smyth, A. R.; Veríssimo, D. Scientific Evidence Supports a Ban on Microbeads. *Environ. Sci. Technol.* **2015**, *49* (18), 10759–10761.
(24) Hanke, G.; Galgani, F.; Werner, S.; Oosterbaan, L.; Nilsson, P.; Fleet, D.; Kinsey, S.; Thompson, R.; Palatinus, A.; Franeker, J. A. Van; et al. *MSFD GES technical subgroup on marine litter. Guidance on monitoring of marine litter in European Seas.*; Luxembourg, 2013.
(25) Hidalgo-Ruz, V.; Gutow, L.; Thompson, R. C.; Thiel, M. Microplastics in the Marine Environment: A Review of the Methods Used for Identification and Quantification. *Environ. Sci. Technol.* **2012**, *46*, 3060−3075.
(26) Lavers, J. L.; Oppel, S.; Bond, A. L. Factors influencing the detection of beach plastic debris. *Mar. Environ. Res.* **2016**, *119*, 245–251.
(27) Andrady, A. L. Using flow cytometry to detect micro- and nano-scale polymer particles. In *Proceedings of the Second Research Workshop on Microplastic Debris.*; Arthur, C., Baker, J., Eds.; NOAA Technical Memorandum NOS-OR&R-39., 2010.
(28) Shim, W. J.; Song, Y. K.; Hong, S. H.; Jang, M. Identification and quantification of microplastics using Nile Red staining. *Mar. Pollut. Bull.* **2016**, *113*, 469–476.
(29) Cole, M. A novel method for preparing microplastic fibers. *Sci. Rep.* **2016**, *6*, 34519.
(30) Rumin, J.; Bonnefond, H.; Saint-Jean, B.; Rouxel, C.; Sciandra, A.; Bernard, O.; Cadoret, J.-P.; Bougaran, G. The use of fluorescent Nile red and BODIPY for lipid measurement in microalgae. *Biotechnol. Biofuels* **2015**, *8*, 42.
(31) Claessens, M.; Van Cauwenberghe, L.; Vandegehuchte, M. B.; Janssen, C. R. New techniques for the detection of microplastics in sediments and field collected organisms. *Mar. Pollut. Bull.* **2013**, *70* (1–2), 227–233.
(32) Tagg, A. S.; Sapp, M.; Harrison, J. P.; Ojeda, J. J. Identification and Quantification of Microplastics in Wastewater Using Focal Plane Array-Based Reflectance Micro-FT-IR Imaging. *Anal. Chem.* **2015**, *87* (12), 6032–6040.
(33) Zimmermann, W.; Paterson, A.; Broda, P. Preparation of Milled Straw Lignin from Barley. *Methods Enzymol.* **1988**, *161*, 191–199.
(34) Nuelle, M.-T.; Dekiff, J. H.; Remy, D.; Fries, E. A new analytical approach for monitoring microplastics in marine sediments. *Environ. Pollut.* **2014**, *184*, 161–169.
(35) Team, R. C. R Core Team 2015 R: A language and environment for statistical computing. R foundation for statistical computing. **2015**, 2014.
(36) Liland, K. H.; Mevik, B.-H.; Canteri, R. baseline: Baseline Correction of Spectra. 2015.
(37) Gillespie, C. S. Fitting heavy tailed distributions: the poweRlaw package. *J. Stat. Softw.* **2015**, *64* (2), 1–16.
(38) Clauset, A.; Shalizi, C. R.; Newman, M. E. J. Power-Law distributions in empirical data. *Soc. Ind. Appl. Math.* **2009**, *51* (4), 661–703.
(39) Wickham, H. *ggplot2*; Gentleman, R., Hornik, K., Parmigiani, G., Eds.; Springer, 2009.
(40) Lenz, R.; Enders, K.; Stedmon, C. A.; Mackenzie, D. M. A.; Gissel, T. A critical assessment of visual identification of marine microplastic using Raman spectroscopy for analysis improvement. *Mar. Pollut. Bull.* **2015**, *100* (1), 82–91.
(41) Ballent, A.; Corcoran, P. L.; Madden, O.; Helm, P. A.; Longstaffe, F. J. Sources and sinks of microplastics in Canadian Lake Ontario nearshore, tributary and beach sediments. *Mar. Pollut. Bull.* **2016**, *110* (1), 383–395.
(42) Maes, T.; Jessop, R.; Wellner, N.; Haupt, K.; Mayes, A. G. A rapid-screening

approach to detect and quantify microplastics based on fluorescent tagging with Nile Red. *Sci. Rep.* **2017**, *7*, 44501.
(43) Dodbiba, G.; Haruki, N.; Shibayama, A.; Miyazaki, T.; Fujita, T. Combination of sink–float separation and flotation technique for purification of shredded PET-bottle from PE or PP flakes. *Int. J. Miner. Process.* **2002**, *65*, 11–29.
(44) Cole, M.; Webb, H.; Lindeque, P. K.; Fileman, E. S.; Halsband, C.; Galloway, T. S. Isolation of microplastics in biota-rich seawater samples and marine organisms. *Sci. Rep.* **2014**, *4*, 4528.
(45) Löder, M. G. J.; Kuczera, M.; Mintenig, S.; Lorenz, C.; Gerdts, G. Focal plane array detector-based micro-Fourier-transform infrared imaging for the analysis of microplastics in environmental samples. *Environ. Chem.* **2015**, *12* (5), 563–581.
(46) Frère, L.; Paul-Pont, I.; Moreau, J.; Soudant, P.; Lambert, C.; Huvet, A.; Rinnert, E. A semi-automated Raman micro-spectroscopy method for morphological and chemical characterizations of microplastic litter. *Mar. Pollut. Bull.* **2016**, *113* (1–2), 461–468.
(47) PlasticsEurope. *Plastics - the facts 2015*; Brussels, 2015.
(48) Phuong, N. N.; Zalouk-Vergnoux, A.; Poirier, L.; Kamari, A.; Châtel, A.; Mouneyrac, C.; Lagarde, F. Is there any consistency between the microplastics found in the field and those used in laboratory experiments? *Environ. Pollut.* **2016**, *211*, 111–123.
(49) Long, M.; Moriceau, B.; Gallinari, M.; Lambert, C.; Huvet, A.; Raffray, J.; Soudant, P. Interactions between microplastics and phytoplankton aggregates: Impact on their respective fates. *Mar. Chem.* **2015**, *175*, 39–46.
(50) Zhao, S.; Danley, M.; Ward, J. E.; Mincer, T. J. An approach for extraction, characterization and quantitation of microplastic in natural marine snow using Raman microscopy. *Anal. Methods* **2017**, *9*, 1470–1478.
(51) Eriksen, M.; Thiel, M.; Lebreton, L. Nature of Plastic Marine Pollution in the Subtropical Gyres. In *The Handbook of Environmental Chemistry*; Takada, H., Karapanagioti, H. K., Eds.; Springer Berlin Heidelberg, 2016; pp 1–28.
(52) Enders, K.; Lenz, R.; Stedmon, C. A.; Nielsen, T. G. Abundance, size and polymer composition of marine microplastics ≥ 10 μ m in the Atlantic Ocean and their modelled vertical distribution. *Mar. Pollut. Bull.* **2015**, *100*, 70–81.
(53) Filella, M. Questions of size and numbers in environmental research on microplastics: Methodological and conceptual aspects. *Environ. Chem.* **2015**, *12* (5), 527–538.

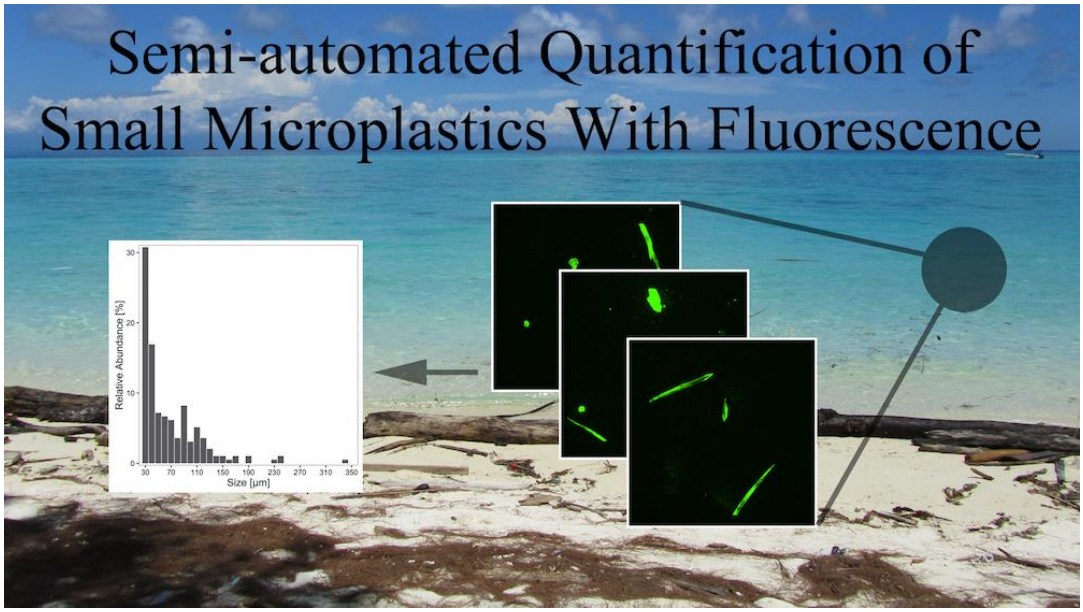
Semi-automated Quantification of
Small Microplastics With Fluorescence
Relative Abundance [%]
Size [µm]

592
593
594

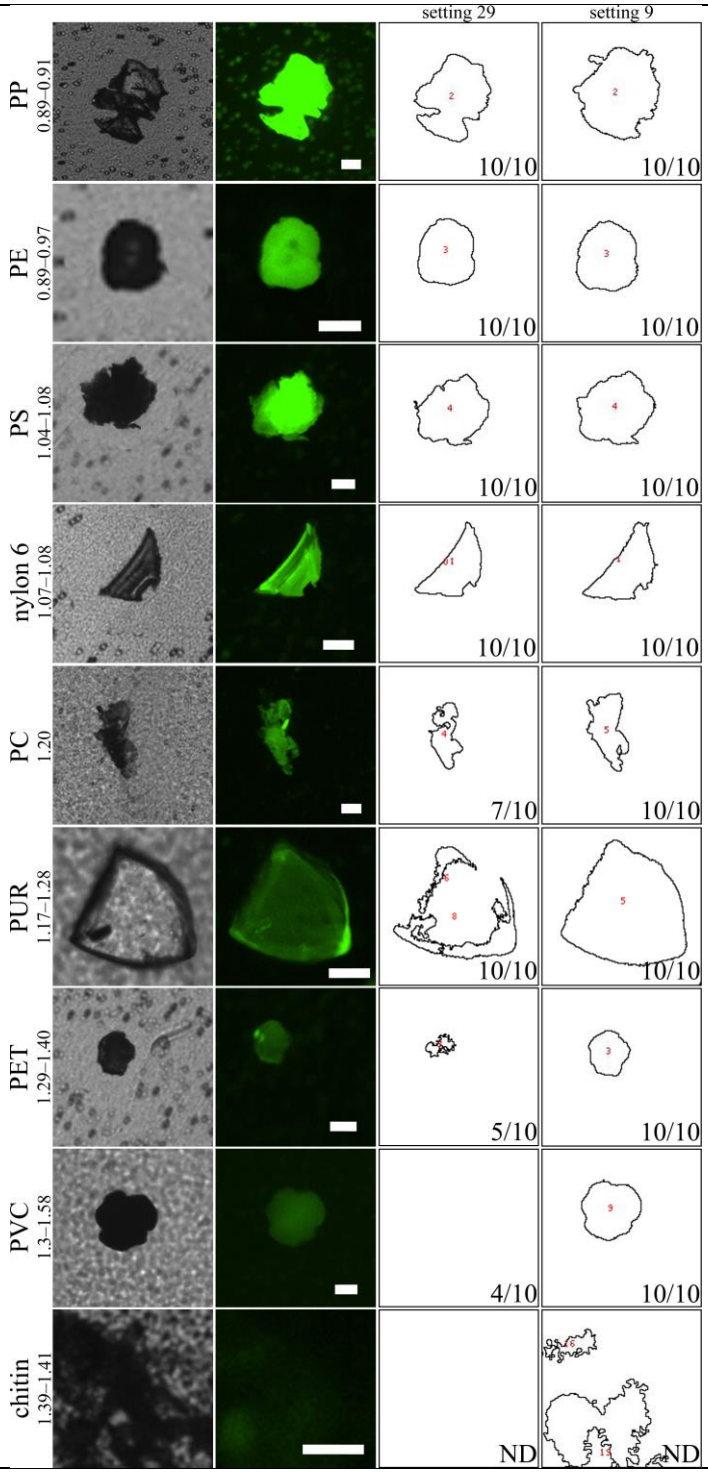

Figure 1. Microscope and ImageJ images of microparticles of different polymer types on PCTE filter membranes stained with Nile red. For each polymer, images show from left to right: a particle in brightfield, the same particle in green fluorescence (excitation/emission 460/525 nm), ImageJ rendition with stringent settings (setting 29) and ImageJ rendition with more sensitive settings (setting 9). Ratios in ImageJ renditions indicate the number of particles (n = 10) detected with the respective setting and polymer; ND: not determined. Polymers are in descending order in accordance with increasing specific density (g/cm^3), indicated below polymer name; PP: polypropylene, PE: polyethylene, PS: polystyrene, PC: polycarbonate, PUR: polyurethane, PET: poly(ethylene therephthalate), PVC: poly(vinyl carbonate). Scale = 50 µm.

595

596

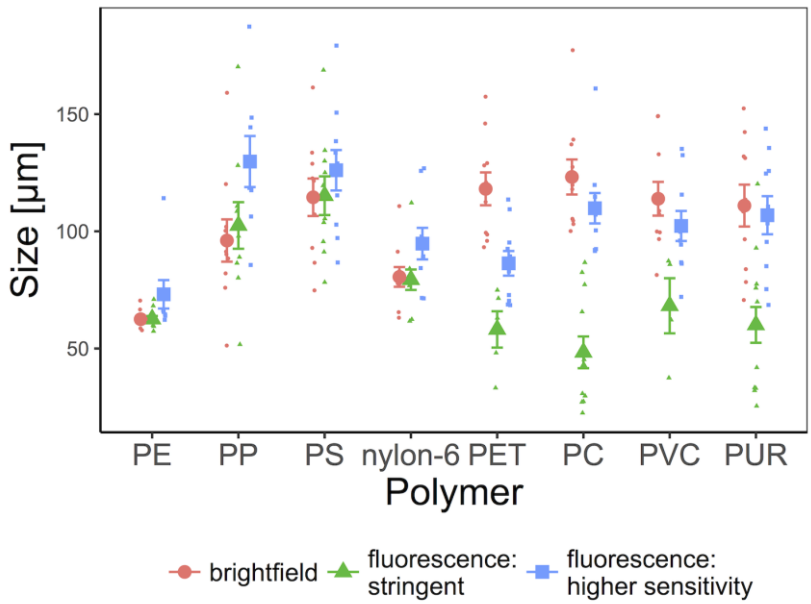

Figure 2. Mean size (± SE) comparison of microplastic particle (n = 10 per polymer type) size measured in ImageJ using either brightfield images or green fluorescence images with our script. Note: *stringent* represents sizes measured with 29 as the lower threshold for pixel brightness and *higher sensitivity* corresponds to measurements generated with 9 as the lower threshold for pixel brightness. Size corresponds to the square root of particle area.

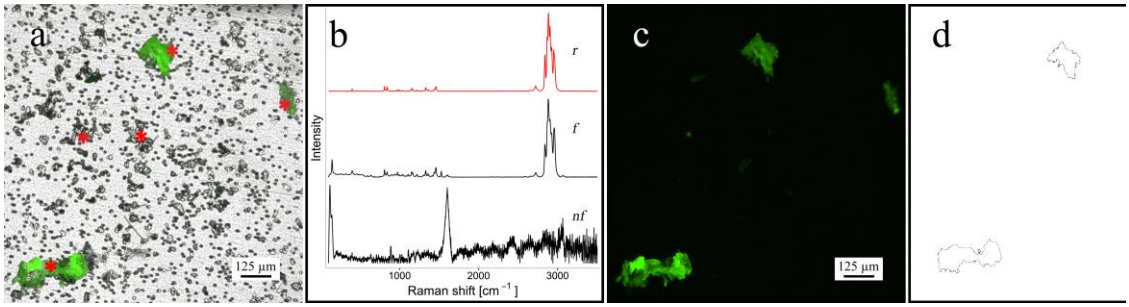

Figure 3. Microscope images of processed sand samples demonstrating selective Nile red fluorescent staining of synthetic polymers with Raman spectra of scanned particles. (a) Composite image of excitation/emission 460/525 nm and brightfield. Asterisks indicate particles assessed via Raman-spectroscopy. (b) Normalised Raman spectra obtained from particles highlighted in image b. *r*: PP (Sigma-Aldrich) spectrum; *f*: typical spectrum of fluorescent particle in image b; *nf*: typical spectrum of non-fluorescing particle in image b. (c) Field shown in panel (a) using green fluorescence only. (d) ImageJ drawing depicting particles >400 µm^2 that were quantified *via* our macro.

599
600

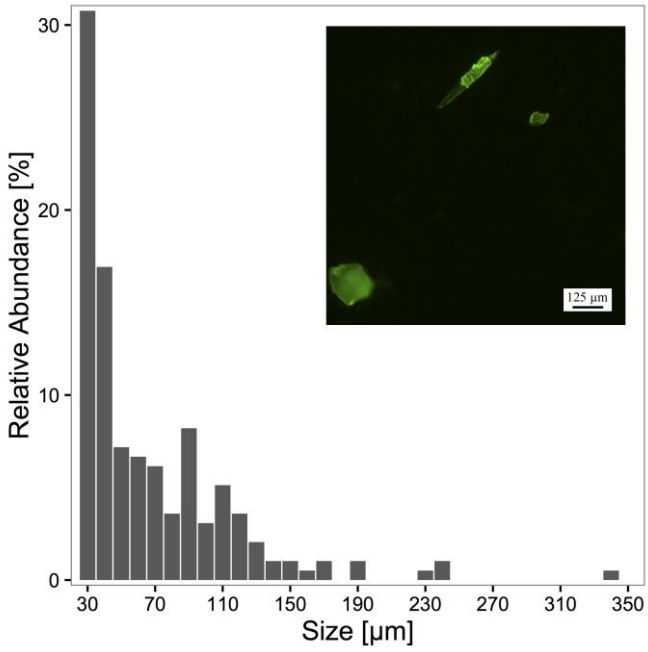

Figure 4. Relative abundance of microplastic particle sizes (n_p = 199) from all sea surface samples analysed via automated counting of fluorescent particles using 109 different microscope fields (one image shown as example). Size corresponds to the square root of the particle's area.

601